High-Resolution Multinuclear NMR Structural Study of Binary Aluminosilicate and Other Related Glasses

S. Sen* and R. E. Youngman

Glass Research Division, Corning Incorporated, Corning, New York 14831

Received: December 31, 2003; In Final Form: March 20, 2004

The structure of homogeneous binary $SiO_2-Al_2O_3$ glasses with 0.4 to up to 12.0 wt % Al_2O_3 have been studied using high-resolution ^{27}Al, ^{17}O, and ^{29}Si NMR spectroscopic techniques. All glasses are found to contain a mixture of 4-, 5-, and 6-fold coordinated Al sites (Al^{IV}, Al^{V}, and Al^{VI}). The relative proportions of these sites are strongly dependent on composition with Al^{IV} (Al^{V}) being most dominant in glasses with <1 wt % (≥ 7 wt %) Al_2O_3. On the other hand, no significant dependence of Al speciation on fictive temperature is observed. The coordination polyhedra of a significant fraction of the Al^{VI} sites in these glasses are found to be unusually distorted, similar to that in the case of crystalline Al_2SiO_5 polymorphs. The ^{17}O NMR spectra show the presence of three types of oxygen sites, Si−O−Al^{V}, Si−O−Al^{IV}, and Si−O−Si, in these glasses. The ^{29}Si MAS NMR spectra corroborate these results and reveal the presence of Q^4 sites with and without Al next-nearest neighbors. It is hypothesized that the tetrahedral $[AlO_{4/2}]^{-1}$ units in glasses with <1 wt % Al_2O_3 are predominantly charge balanced by the formation of oxygen triclusters, whereas the Al^{V} and Al^{VI} sites play the role of charge compensators in glasses with higher Al content. Addition of either low field strength alkali ions such as K^+ or high field strength rare earth ions such as La^{3+} to these glasses results in charge balance and stabilization of Al^{IV} sites.

Introduction

Glasses in the binary system $Al_2O_3-SiO_2$ are of significant technological importance in the areas of high-temperature ceramics and rare earth doped fiber optic amplifiers for all-optical telecommunication networks.[1−3] The atomic structure of these glasses is also interesting from a fundamental point of view, as the structural role of Al in binary $Al_2O_3-SiO_2$ glasses remains controversial, especially in relation to the charge balancing mechanisms of tetrahedral $[AlO_{4/2}]^{-1}$ units.[4] Previous structural studies with ^{27}Al magic-angle-spinning (MAS) nuclear magnetic resonance (NMR) spectroscopy of rapidly quenched binary $Al_2O_3-SiO_2$ glasses with 10−72 wt % Al_2O_3 have indicated the presence of Al in 4-, 5-, and 6-fold coordination with oxygen (Al^{IV}, Al^{V}, and Al^{VI}).[5−9] Unfortunately the ^{27}Al MAS NMR spectra of these glasses tended to be broad with strongly overlapping signals from multiple Al environments, and most of these glasses were phase-separated and/or partially crystallized, thus making the structural interpretations difficult. It has been conjectured on the basis of these NMR results that one of the immiscible phases in these glasses is silica-rich with Al mostly as Al^{IV} and the other phase is alumina-rich with Al being present as a mixture of Al^{IV}, Al^{V}, and Al^{VI}. On the other hand ^{27}Al NMR studies of $Al_2O_3-SiO_2$ glasses made by sol−gel techniques show that the Al coordination environment is strongly dependent on the processing route, indicating that sol−gel derived glasses are perhaps not in thermodynamic equilibrium.[10,11] Homogeneous glasses with low Al_2O_3 content ($\sim$0.7 wt %) have been studied with Al K-edge extended X-ray absorption fine structure (EXAFS) spectroscopy.[1] Although the EXAFS results indicate that the majority of the Al are present in 4-fold coordinated state in these glasses, the technique itself is not well-suited for studying mixed coordination environments in glasses. On the other hand electron paramagnetic resonance (EPR) spectroscopic results on electrically fused natural quartz with 10−50 ppm by weight Al indicate the presence of 3-fold coordinated Al^{3+} ions in silica.[12] However, it must be noted that EPR only observes a minor fraction of the Al environments in the glass, namely, those that have paramagnetic centers associated with them. In situ ^{27}Al NMR spectroscopic studies of $Al_2O_3-SiO_2$ liquids at temperatures above their melting point have indicated a composition-dependent change in the average coordination number of Al, although the true nature of the structural change has remained unclear.[8] Molecular dynamics simulations of $Al_2O_3-SiO_2$ liquids by the same authors have indicated a decrease in the concentration of Al^{V} and Al^{VI} species and a concomitant increase in Al^{IV} with increasing SiO_2 content.[8]

In the present work we report the results of a detailed study of the short-range atomic structure of homogeneous binary $Al_2O_3-SiO_2$ glasses with 0.4−12.0 wt % Al_2O_3 using high-resolution ^{27}Al, ^{29}Si, and ^{17}O NMR spectroscopic techniques. The key questions that have been addressed in this study are the compositional dependence of the Al coordination environments and the charge balance mechanism of the tetrahedral $[AlO_{4/2}]^{-1}$ units in these binary glasses. The role of alkali and rare earth ions in controlling the coordination behavior of Al as charge-balancing cations is discussed. Some high-resolution ^{27}Al NMR results on phase-separated glasses with Al_2O_3 contents ranging between 20 and 40 wt % are also presented.

Experimental Section

Sample Preparation. All glasses were prepared in 2−5 g batches by conventional melt quenching method. The batch materials used in glass melting were ultrahigh purity silica (99.999%), γ-Al_2O_3 (99.999%), K_2CO_3 (99.99%), and La_2O_3 (99.99%). The batch materials were finely crushed in an agate mortar, contained in 80% Pt/20% Rh crucibles, and melted at

10.1021/jp031348u CCC: $27.50
Published on Web 05/07/2004

1800 °C for 6 h in a furnace (Deltech DT-33-CVT-912) in air. These melts were cooled in air, and the resulting glasses were finely crushed, remelted for another 4 h at 1800 °C to ensure chemical homogeneity, and finally quenched in water. All glass samples were completely colorless and did not show any visual indication of phase separation even in binary aluminosilicate glasses with up to 40 wt % Al_2O_3. Glasses with ≤15 wt % Al_2O_3 contained a large number of bubbles; however, completely inclusion-free glass was obtained at higher Al_2O_3 contents, presumably as a result of sufficient lowering of the viscosity of the corresponding melts on addition of alumina. The ^{17}O-enriched glasses were synthesized using ^{17}O-enriched SiO_2 and were doped with 0.1 wt % Gd_2O_3 to shorten the ^{17}O NMR spin−lattice relaxation time. The ^{17}O-enriched SiO_2 was prepared by hydrolyzing $SiCl_4$ with 80% enriched $H_2{}^{17}O$.[13] The ^{17}O-enriched glasses were melted in a flowing Ar atmosphere to avoid loss of ^{17}O by isotopic exchange with the oxygen in air. The chemical compositions of all glasses as reported here were analyzed with standard electron probe microanalysis (EPMA) technique. All glasses were found to be chemically homogeneous over length scales of a few micrometers, the latter being limited by the resolution of the EPMA technique.

Scanning Electron Microscopy. The binary aluminosilicate glasses were examined for phase separation using a field emission scanning electron microscope (LEO 1550VP). Specimens for SEM were prepared from small pieces of glass samples that were ground, polished, and etched for 2 min in 2.5% HF to enhance the compositional heterogeneity through differential etching. Images were then taken at 25,000X and 75,000X magnification with an in-lens secondary detector operating at an accelerating potential of 5 kV. Representative electron micrographs for three glasses with 12, 20, and 40 wt % Al_2O_3 are shown in Figure 1. All glasses with ≤12 wt % Al_2O_3 did not show any sign of phase separation. The first appearance of Al-rich spherical dispersed droplets with diameters of ∼20 nm was observed in glasses with 15−20 wt % Al_2O_3, and further coarsening and formation of interconnected wormlike structure was observed in glasses with ≥30 wt % Al_2O_3 (Figure 1). These results are in complete agreement with previous studies that have shown that phase separation in the nanometer length scale into an alumina-rich and a silica-rich phase becomes observable in binary aluminosilicate glasses at an Al_2O_3 content of ∼15 wt % or higher.[3,5]

NMR Spectroscopy. All ^{27}Al NMR experiments were conducted using a commercial NMR spectrometer (Chemagnetics Infinity) in conjunction with an 11.7 T wide-bore superconducting magnet (Oxford). The resonance frequency of ^{27}Al at this magnetic field was 130.22 MHz. Glass samples were ground using an agate mortar and pestle and subsequently packed into 2.5 mm zirconia rotors. NMR spectra were collected using a 2.5 mm double-resonance MAS NMR probe, with spinning speeds of 26 kHz. ^{27}Al MAS NMR spectra were collected using a background suppression pulse sequence and radio frequency pulse widths of 0.6 μs (less than $\pi/8$). Several thousand to several hundred thousand free induction decays (FID) were signal-averaged using a recycle delay of 0.5 s. Longer delays did not result in appreciably different data. The ^{27}Al MAS NMR data were processed with minimal line broadening (typically less than 500 Hz) and referenced to an external chemical shift standard of aqueous $Al(NO_3)_3$.

^{27}Al triple quantum MAS (3QMAS) NMR spectra were collected using a hypercomplex 3QMAS sequence with a Z filter.[14] The solid $\pi/2$ and $3\pi/2$ pulse widths were optimized to 0.7 and 2 μs, respectively. A pulse width of 15 μs was used as the soft reading pulse of the Z filter. MQMAS data were typically collected using 1 000−50 000 acquisitions at each of 48 t_1 points, with a recycle delay of 0.5−1 s. Spectra were processed and shear transformed using commercial software.

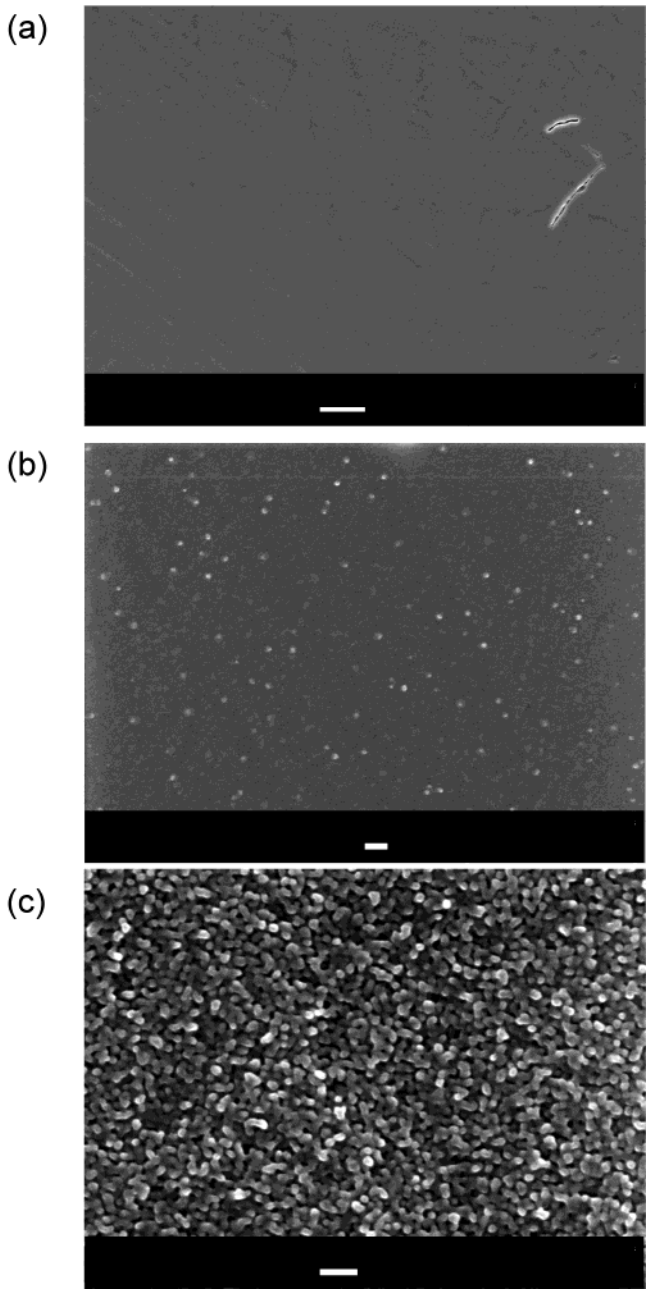

Figure 1. Field emission SEM images of binary aluminosilicate glasses with (a) 12, (b) 20, and (c) 40 wt % Al_2O_3. Al-rich regions show up as white spherical droplets in (b). The length of the white line at the bottom of each micrograph = 100 nm.

^{17}O 3QMAS NMR spectra were also collected at 11.7 T (67.76 MHz resonance frequency), using the same equipment and 3QMAS pulse sequence as described above. ^{17}O-enriched glass samples were powdered and packed into 3.2 mm zirconia rotors. Data were collected using a 3.2 mm double-resonance MAS NMR probe and spinning speeds of typically 20 kHz. The solid $\pi/2$ and $3\pi/2$ pulse widths were optimized to 1 and 3 μs, respectively. The soft reading pulse of the Z filter was optimized to 20 μs, and the filter delay was set to 0.28 ms. Approximately 6000 scans were collected for each of 60 t_1 values, using a recycle delay of 0.7 s. ^{17}O 3QMAS NMR spectra

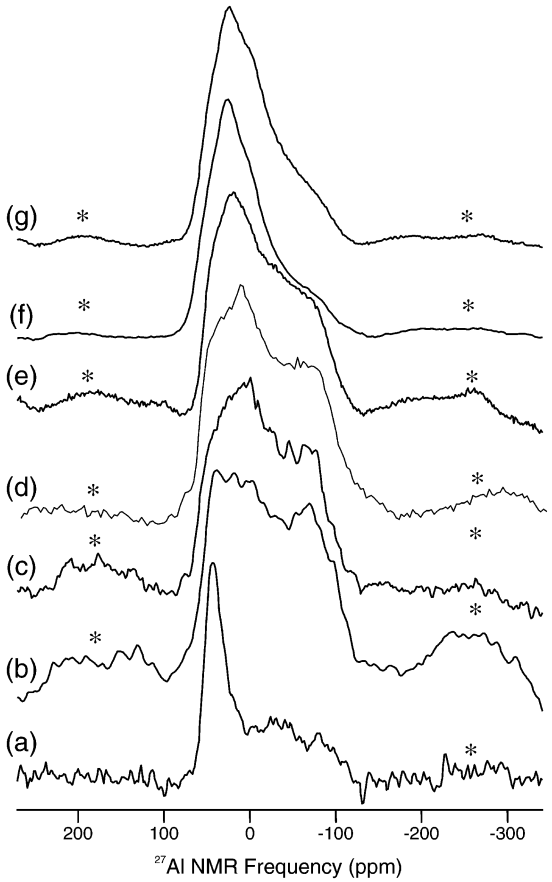

Figure 2. ^{27}Al MAS NMR spectra of homogeneous binary aluminosilicate glasses containing (a) 0.4, (b) 1, (c) 4, (d) 5, (e) 7, (f) 10, and (g) 12 wt % Al_2O_3. Asterisks denote spinning sidebands.

were processed, shear transformed, and plotted against the chemical shift of ^{17}O-enriched H_2O.

^{29}Si MAS NMR spectra were collected at 4.7 T (39.70 MHz resonance frequency) using a commercial spectrometer (Chemagnetics Infinity), wide-bore superconducting magnet (Oxford), and a 9.5 mm MAS NMR probe. Glass samples were crushed and loaded into 9.5 mm zirconia rotors, and a nominal spinning speed of 4.5 kHz was used. $\pi/4$ pulse widths (typically 3 μs) and recycle delays of 180 s were used to acquire from 10 000 to 100 000 scans. ^{29}Si NMR spectra were processed with approximately 100 Hz line broadening and plotted against the chemical shift of tetramethylsilane (TMS).

Results

^{27}Al NMR. The ^{27}Al MAS NMR spectra of the homogeneous binary $Al_2O_3-SiO_2$ glasses are shown in Figure 2. It is immediately clear from Figure 2 that the ^{27}Al MAS NMR spectra and therefore the Al coordination environments in these glasses are dependent on composition. At low Al concentration levels (<1 wt % Al_2O_3) the ^{27}Al MAS NMR spectra largely consist of a narrow peak centered at ca. +50 ppm, indicating that most of the Al is in 4-fold coordination (Figure 2).[5] With further increase in Al concentration the ^{27}Al NMR signals broaden significantly with increased intensities in the lower frequency region near ca. +30 and 0 ppm indicating a corresponding increase in the relative concentrations of high-coordinated Al^V and Al^{VI} species.[5] It is important to note that all of these ^{27}Al MAS NMR line shapes also have significant intensity in the chemical shift range between 0 and −100 ppm that is rather unusual for Al in oxide glasses and crystals.[15] This feature is most prominent in glasses with Al_2O_3 contents ranging between 1 and 7 wt % (Figure 2). A quantitative interpretation of these ^{27}Al MAS NMR spectra is severely complicated by the presence of second-order quadrupolar broadening in the corresponding line shapes with multiple, strongly overlapping peaks.

Al quantitation experiments were carried out to determine the amount of ^{27}Al NMR signal detected in these MAS NMR experiments. The ^{27}Al MAS NMR signal obtained from a known quantity of each glass was compared to that obtained from a known quantity of a crystalline standard, in this case, 99.99% pure hexagonal $AlPO_4$ using identical pulse sequence and acquisition parameters. The spectra were processed without any line broadening and integrated over a sufficiently large range to include the first set of spinning sidebands, typically from +250 to −250 ppm. These experiments indicate that all of the Al NMR signal is detected for glasses with low (<1 wt %) and high (>7 wt %) Al_2O_3 contents. At intermediate Al_2O_3 contents (between 1 and 7 wt %) ~75% of the total Al is detected in the ^{27}Al MAS NMR signal. The loss of some ^{27}Al NMR signal from these compositions is due mainly to the receiver dead-time, during which some signal from very broad ^{27}Al MAS NMR line shapes corresponding to distorted Al coordination environments with large nuclear quadrupolar coupling constants may be lost. It is interesting to note that the ^{27}Al MAS NMR spectra of the glass compositions for which some Al signal is lost are also characterized by a high relative intensity of the very broad spectral feature between 0 and −100 ppm, as discussed above.

Further enhancement in the resolution of the ^{27}Al NMR signal from multiple coordination environments in these binary aluminosilicate glasses can be obtained by using the 3QMAS NMR spectroscopic technique. This two-dimensional NMR spectroscopic technique averages out the second-order quadrupolar line broadening effects for quadrupolar nuclides such as ^{27}Al by mixing single and triple quantum coherences to generate an isotropic spectrum in one dimension; this spectrum is correlated with the single-quantum MAS central transition spectrum in the second dimension.[16] The high-resolution spectrum in the isotropic dimension is only broadened by the distributions of chemical shift and quadrupolar coupling constants. Figure 3 shows representative contour plots of the ^{27}Al 3QMAS NMR spectra and their total projections in the isotropic dimension for three binary aluminosilicate glasses with 5, 10, and 12 wt % Al_2O_3. These spectra clearly resolve the presence of all three of the Al^{IV}, Al^V, and Al^{VI} species that coexist in these glasses with isotropic dimension shifts of ca. 73, 44 and 13 ppm, respectively (Figure 3). The glass with 5 wt % Al_2O_3 contains mainly Al^{IV} and Al^{VI} with Al^V as the minor species. A similar Al speciation is expected to be present in glasses with Al_2O_3 concentrations ranging between 1 and 7 wt % on the basis of the similarity between the corresponding ^{27}Al MAS spectra (Figure 2). On the other hand the glasses with 10 and 12 wt % Al_2O_3 contain principally Al^{IV} and Al^V with a small fraction of Al^{VI} (Figure 3). This trend in Al speciation is observed to continue in phase-separated glasses with Al_2O_3 contents of up to 40 wt % (vide infra). The isotropic chemical shifts and quadrupolar coupling constants (C_q) for the Al^{IV}, Al^V, and Al^{VI} species can be calculated from the 3QMAS NMR spectra using the procedures described by Amoureux et al.[17] For each resonance in the 3QMAS NMR spectrum, the centers of gravity in the MAS and isotropic dimensions, δ_2^{CG} and δ_{iso}^{CG}, are used to

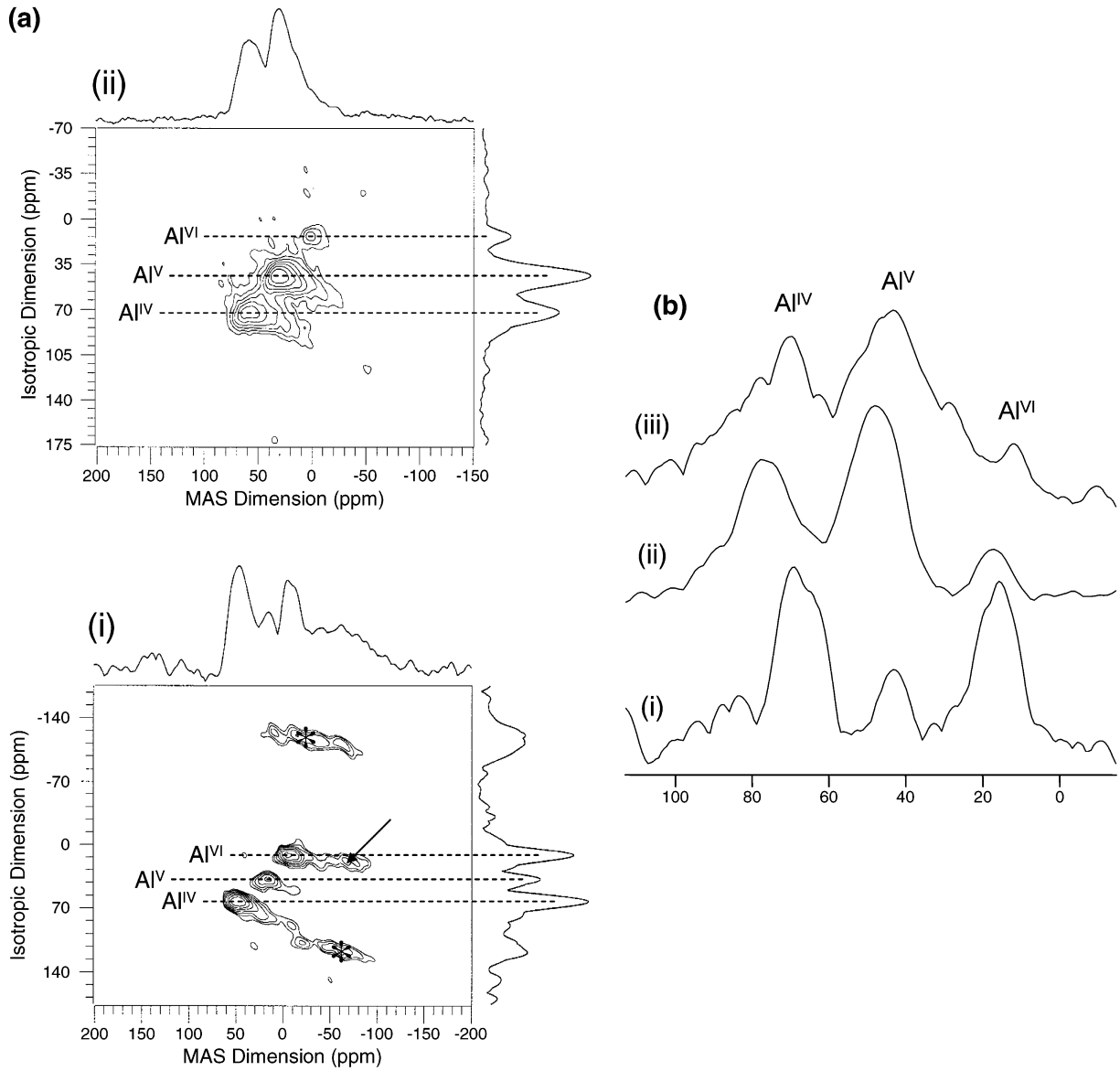

Figure 3. (a) Two-dimensional ^{27}Al 3QMAS NMR spectra of binary aluminosilicate glasses containing (i) 5 and (ii) 10 wt % Al_2O_3. Horizontal and vertical frequency axes correspond to MAS and isotropic frequencies, respectively. MAS and isotropic projections are plotted to the top and right of each spectrum, respectively. The arrow in (i) denotes a spectral feature represented by contours elongated parallel to the MAS dimension that corresponds to distorted octahedral sites in this glass (for details see text). Asterisks denote the corresponding spinning sidebands. (b) Isotropic projections of the ^{27}Al 3QMAS NMR spectra of binary aluminosilicate glasses containing (i) 5, (ii) 10, and (iii) 12 wt % Al_2O_3.

calculate the isotropic chemical shift (δ_{CS}) and the quadrupolar coupling product (P_q) according to

$$\delta_{CS} = \frac{10}{27}\delta_2^{CG} + \frac{17}{27}\delta_{iso}^{CG} \quad (1)$$

and

$$P_q = (\delta_{iso}^{CG} - \delta_2^{CG})^{1/2} \cdot f(S) \cdot \nu_0 \cdot 10^{-3} \quad (2)$$

where $f(S) = 10.244$ for nuclides with $I = 5/2$.[17] It is assumed in the subsequent discussion that the quadrupolar asymmetry parameter $\eta = 0$ for these aluminum polyhedra and therefore $P_q = C_q$, although more rigorously $P_q = C_q(1 + \eta^2/3)^{1/2}$. Since η can vary between 0 and 1, such an assumption yields the lower bound for C_q, whereas the upper bound would be a value that is 15% higher, corresponding to $\eta = 1$. The calculated chemical shifts range between 55.5 and 65.0 ppm for the Al^{IV} species, between 29.0 and 38.3 ppm for the Al^{V} species, and between 4.5 and 9.0 ppm for the Al^{VI} species in these glasses. The corresponding ranges of C_q values for the Al^{IV}, Al^{V}, and Al^{VI} species are 5.4−6.6 MHz, 5.1−6.1 MHz, and 4.5−4.8 MHz, respectively. Besides the resolution of the more typical Al^{IV}, Al^{V}, and Al^{VI} species the contour plot of the ^{27}Al 3QMAS spectrum of the glass with 5 wt % Al_2O_3 also resolves a peak elongated parallel to the MAS dimension (Figure 3) that clearly corresponds to the broad spectral feature between 0 and −100 ppm in the corresponding ^{27}Al MAS NMR spectrum (Figures 2 and 3). The isotropic chemical shift and C_q for this Al site are found to be −8.4 ppm and 10.8 MHz, respectively.

The ^{27}Al MAS NMR spectra of three aluminosilicate glasses with different K_2O contents are shown in Figure 4. The ^{27}Al MAS NMR line shape shows tremendous narrowing and simplification on addition of K_2O. In the absence of K_2O the ^{27}Al MAS line shape is broad and contains signals from all three of the Al^{IV}, Al^{V}, and Al^{VI} species as discussed above (Figure 4). On the other hand the ^{27}Al MAS NMR spectrum of the glass with a K/Al ratio of ca. 0.5 largely consists of a relatively narrow resonance at ca. +60 ppm characteristic of Al^{IV} species (Figure

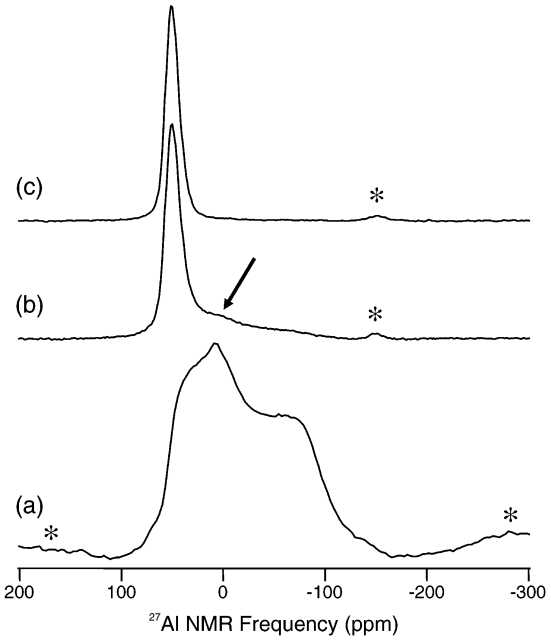

Figure 4. ^{27}Al MAS NMR spectra of (a) a binary aluminosilicate glass with 5 wt % Al_2O_3, (b) a peraluminous potassium aluminosilicate glass with 4.14 mol % Al_2O_3 and 2 mol % K_2O, and (c) a charge-balanced potassium aluminosilicate glass with 3.07 mol % each of Al_2O_3 and K_2O. Spinning sidebands are marked with asterisks, and the arrow denotes a weak nontetrahedral aluminum resonance in the peraluminous glass.

4). However, a broad low-intensity component with a line shape similar to that of the K-free glass is also apparent in this spectrum. Finally, only Al^{IV} species are observed in the ^{27}Al MAS NMR spectrum on further addition of K_2O such that K/Al $\approx$ 1 (Figure 4). The ^{27}Al MAS spectrum of a binary aluminoslicate glass with ca. 4.0 mol % Al_2O_3 is compared in Figure 5 with that of a glass with ca. 4.0 mol % Al_2O_3 and 1.0 mol % La_2O_3. These spectra clearly indicate that the addition of La has an effect similar to that of K in narrowing the ^{27}Al MAS line shape, which is indicative of a lowering in the relative concentration of Al^V and Al^{VI} species and the distorted Al^{VI} species compared to that of the Al^{IV} species. The ^{27}Al 3QMAS NMR spectrum of the La−Al glass unequivocally establishes this conjecture, which shows that the Al coordination environment in this glass is dominantly tetrahedral with a small concentration of Al^V species (Figure 5). This observation is in accordance with the results of a previous NMR study of La−Al silicate glasses with La and Al contents significantly higher than those of the one studied here.[18]

^{29}Si MAS NMR. The ^{29}Si MAS NMR spectra of the binary aluminosilicate glasses are shown in Figure 6. It is clear from these spectra that the primary effect of progressive addition of Al to SiO_2 is an increasing asymmetry of the ^{29}Si MAS NMR line shapes with a shift of the center of gravity toward the higher frequency side.

^{17}O 3Q-MAS NMR. The ^{17}O 3QMAS NMR data have been collected for a binary aluminosilicate glass with 10 wt % Al_2O_3 (Figure 7). The contour plot of the 3QMAS NMR spectrum for this glass show clear indication of the presence of multiple oxygen sites. The corresponding peaks in the contour plot are elongated primarily in the MAS dimension, characteristic of bridging oxygen type of environments.[19] The total isotropic projection shows the presence of three resolved bridging oxygen sites with isotropic dimension shifts of 61.3, 43.8, and 33.3 ppm (Figure 7). The strongest peak at an isotropic dimension shift of 61.3 ppm has an isotropic chemical shift of 40.4 ppm and a

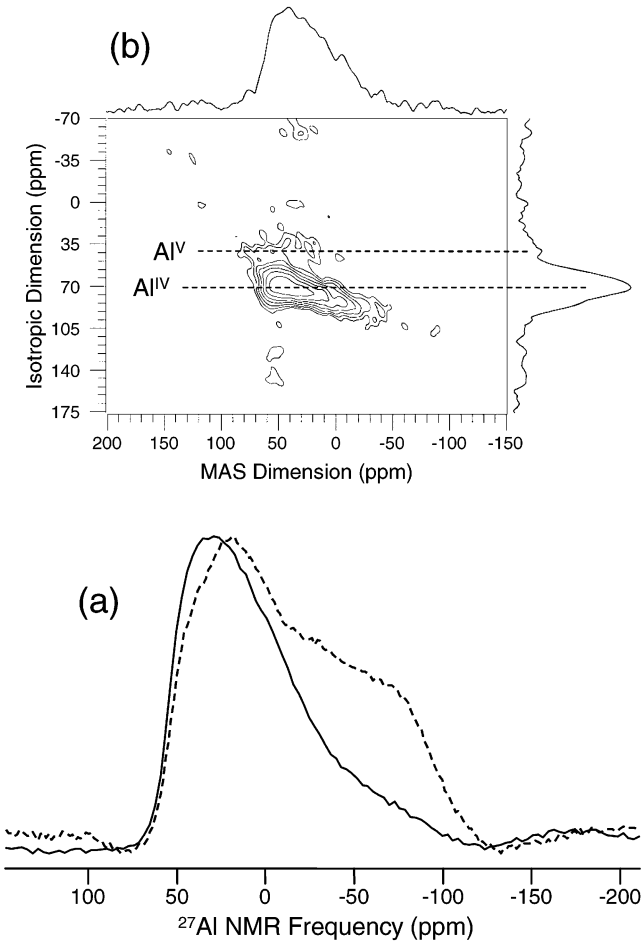

Figure 5. (a) ^{27}Al MAS NMR spectra of a binary aluminosilicate glass with 4 mol % Al_2O_3 (dashed curve) and a ternary lanthanum aluminosilicate glasses containing 4 mol % Al_2O_3 and 1 mol % La_2O_3 (solid curve). The ^{27}Al 3QMAS NMR spectrum of this lanthanum aluminosilicate glass is plotted in (b). MAS and isotropic projections are plotted to the top and right of the two-dimensional spectrum, respectively.

C_q of ca. 5.21 MHz and can readily be assigned to the Si−O−Si type of bridging oxygens on the basis of its typical C_q and relative abundance.[20,21] The relatively weak second peak at a lower isotropic dimension shift of 43.8 ppm is characterized by an isotropic chemical shift of 32.3 ppm and a C_q of ca. 3.87 MHz, both typical of bridging oxygens of the type Si−O−Al^{IV}.[20,21] Since the ^{27}Al 3QMAS NMR data reveal the presence of mainly $Al^{IV}$and Al^V species in this binary glass (Figure 3), the third ^{17}O peak with an isotropic dimension shift of 33.3 ppm can be assigned to bridging oxygens in Si−O−Al^V type of linkages (Figure 7). The corresponding isotropic chemical shift and C_q for this peak are 24.1 ppm and 3.53 MHz, respectively. It is interesting to note that the ^{17}O 3QMAS spectrum for this glass in Figure 7 does not show any evidence for the presence of typical nonbridging oxygens and Al−O−Al sites in this glass. These types of oxygen sites are characterized by peaks that have a slope of −31/17 in a 3QMAS NMR contour plot and are elongated in the direction of constant C_q but varying isotropic chemical shift.[19] Moreover, typically the Al−O−Al type of oxygen sites are characterized by significantly smaller C_q values (2.3 to 2.7 MHz) than those observed here.

Discussion

The ^{27}Al MAS and 3QMAS NMR results reported here clearly indicate that the coordination environments of Al in the

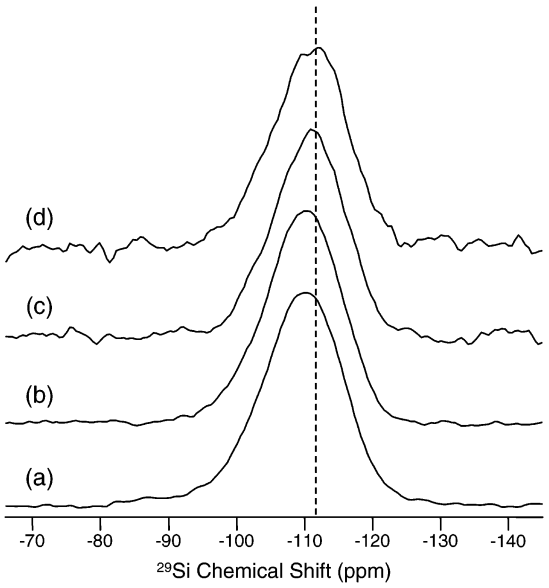

Figure 6. ^{29}Si MAS NMR spectra of binary aluminosilicate glasses containing (a) 10, (b) 5, (c) 2.5, and (d) 1 wt % Al_2O_3. The dashed line marks the chemical shift of Q^4 tetrahedra in pure silica (ca. −112 ppm).

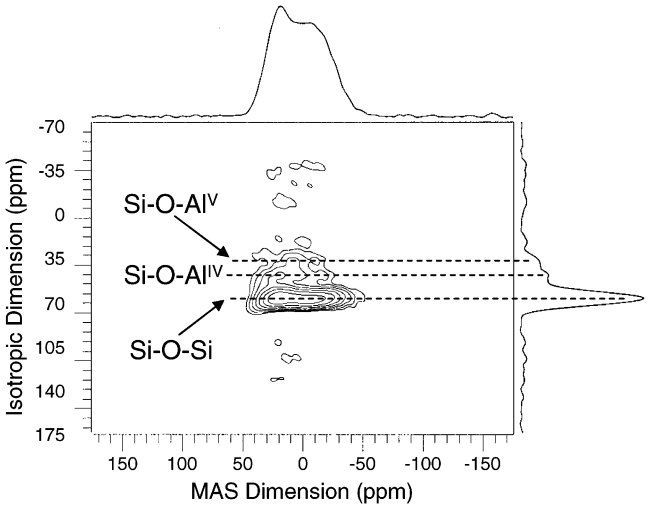

Figure 7. Two-dimensional ^{17}O 3QMAS NMR spectrum of a binary aluminosilicate glasses with 10 wt % Al_2O_3. MAS and isotropic projections are shown to the top and right of the spectra, respectively.

homogeneous binary aluminosilicate glasses are a strong function of composition (Figures 2 and 3). The Al atoms are predominantly tetrahedrally coordinated in glasses with <1 wt % Al_2O_3. This result is in accordance with previous Al K-edge EXAFS spectroscopic results on a binary aluminosilicate glass with ca. 0.7 wt % Al_2O_3 which showed the presence of only Al^{IV} sites.[1] This observation implies that the charge compensation mechanism for every tetrahedral $[AlO_{4/2}]^{-1}$ unit has to involve the formation of a "tricluster" where triply coordinated oxygen atoms are shared by three $Al(Si)O_4$ tetrahedral units.[3,22] Formation of this type of tricluster results in an overconnected and therefore a dense and constrained tetrahedral network. In fact the connectivity of such a network in terms of its average coordination number is going to be even higher than that of silica, which is usually thought to be the oxide network with the highest degree of connectivity or average coordination number. This structural scenario is consistent with the observation made in a previous study of an anomalous increase in the viscosity of silica on doping with a few tens of ppm by weight

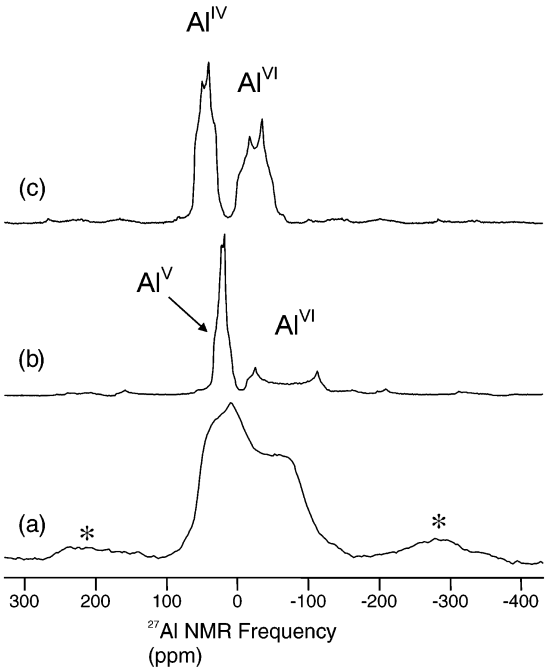

Figure 8. ^{27}Al MAS NMR spectra of (a) a binary aluminosilicate glass containing 5 wt % Al_2O_3, (b) andalusite, and (c) sillimanite. Resonances for the various aluminum polyhedra are denoted for the two crystalline polymorphs of Al_2SiO_5. Asterisks denote spinning sidebands.

of Al_2O_3.[23] This type of a dense tetrahedral network is likely to become energetically unstable at ambient pressure with increasing concentration of the triclusters. Thus it is not surprising that further increase in Al content in these binary aluminosilicate glasses results in the formation of high-coordinated Al^{VI} and Al^{V} sites. These high-coordinated Al sites can have excess positive charge on them and therefore in effect can provide charge compensation to the tetrahedral $[AlO_{4/2}]^{-1}$ units in glasses with ≥1 wt % Al_2O_3.[5] This role of high-coordinated Al as charge compensating species for Al^{IV} becomes apparent when addition of conventional charge balancing cations such as alkalis to these glasses results in the rapid disappearance of Al^{VI} and Al^{V} and stabilization of Al^{IV} (Figure 4). The formation of Al^{IV} is also favored over that of Al^{VI} and Al^{V} in aluminosilicate glasses on addition of La (Figure 5). This observation indicates that the well-known effect of homogenization of the spatial distribution of rare earth (RE) ions in silica on codoping with Al may in fact be associated with the charge compensation related coupling between RE and Al.[1,24]

Besides the signal corresponding to the Al^{IV}, Al^{V}, and Al^{VI} species in the chemical shift range between ca. 0 and ca. +60 ppm, the ^{27}Al MAS NMR spectra for all binary aluminosilicate glasses also have significant intensity between ca. 0 and −100 ppm (Figure 2). To our knowledge ^{27}Al MAS NMR signal in the latter range of chemical shifts in oxide materials has only been observed from significantly distorted Al^{VI} sites in two crystalline polymorphs of $Al_2Si_2O_5$, namely, andalusite and sillimanite.[25] The ^{27}Al MAS NMR spectra for sillimanite and andalusite collected in our laboratory using crushed mineral specimens from private collection are shown in Figure 8. The large C_q of ca. 9−16 MHz associated with these distorted Al^{VI} sites that give rise to the broad ^{27}Al MAS NMR line shapes are clearly evident in these spectra (Figure 8).[15,25] A previous structural study has indicated that the principal source of site distortion in these $Al_2Si_2O_5$ polymorphs is the variation in the Al−O bond lengths in the AlO_6 coordination polyhedra.[26] It is therefore likely that such distorted high-coordinated Al sites also

exist in the binary aluminosilicate glasses and are responsible for the broad ^{27}Al MAS NMR signal in the ca. 0 to −100 ppm chemical shift range (Figure 2). The NMR signal from such broad line shape can easily be lost during the deadtime of the probe, as well as due to inefficient excitation of the corresponding sites with large C_q. The latter case would be especially true for ^{27}Al 3QMAS experiments. However, this broad line shape has been successfully observed in the ^{27}Al 3QMAS spectrum of the aluminosilicate glass with 5 wt % Al_2O_3 (Figure 3). The large C_q of this site (10.8 MHz) unequivocally establishes the distorted nature of this Al site as discussed above. The corresponding chemical shift of −8.4 ppm is consistent with this being an octahedral Al^{VI} site.

The changes in the ^{29}Si MAS NMR line shapes in the binary aluminosilicate glasses as a function of composition are consistent with both the formation of Si atoms with Al next-nearest neighbors, i.e., Si−O−Al linkages and the formation of nonbridging oxygens in the structure, on addition of Al (Figure 6). Direct evidence in favor of the formation of Si−O−Al linkages comes from the ^{17}O 3QMAS spectrum of the glass with 12 wt % Al_2O_3 that reveals the presence of Si−O−Al^{IV} and Si−O−$Al^{V/VI}$ sites and indicates the absence of typical nonbridging oxygens (Figure 7). It is interesting to note that predictions can be made on the basis of bond-valence theory that the oxygen atoms in Si−O−$Al^{V/VI}$ linkages in the aluminosilicate glasses are likely to be coordinated to a third Al.[27] These types of triply coordinated oxygen are ubiquitously present in the structure of all three polymorphs of crystalline Al_2SiO_5. The ^{29}Si NMR spectra of the glasses with ≥10 wt % Al_2O_3 have significant intensities in the range of chemical shift values of ca. −90 to −100 ppm, typical of Si with more than one Al next-nearest neighbors (Figure 6).[15] This result is indicative of an onset of subnanometer scale spatial clustering of Al in these glasses, which is consistent with the fact that phase separation in the nanometer scale becomes observable with SEM in glasses with ≥15 wt % Al_2O_3 (Figure 1).

It has been suggested in a previous ^{27}Al MAS NMR study of phase-separated binary aluminosilicates with up to 50 wt % Al_2O_3 that the relative concentrations of Al^{IV}, Al^{V}, and Al^{VI} species change with composition such that the relative concentration of Al^{VI} is higher in glasses with higher Al content.[5] However, such quantification on the basis of ^{27}Al MAS NMR data alone can often become complicated as a result of the presence of second-order quadrupolar broadening in line shapes with multiple, strongly overlapping peaks. We have used ^{27}Al 3QMAS spectroscopy, which is free of second-order quadrupolar broadening effects and provides higher resolution than the simple MAS technique, to study Al speciation in phase-separated aluminosilicate glasses with 20−40 wt % Al_2O_3. The ^{27}Al MAS and 3QMAS NMR spectra of these glasses are shown in Figure 9. The isotropic projections of the ^{27}Al 3QMAS spectra clearly indicate that irrespective of glass composition the relative concentrations of Al^{IV}, Al^{V}, and Al^{VI} species remain essentially the same.

Finally, previous studies have reported observation of cooling rate or fictive temperature dependence of Al speciation in binary aluminosilicate glasses.[6,7] In these studies it was observed that an aluminosilicate glass with 35 wt % Al_2O_3 contained only $Al^{IV}$and Al^{VI} and no detectable amount of Al^{V} when it was cooled at a rate of 10^2-10^3 K s^{-1}. [6,7] On the other hand substantial amount of Al^{V} was observed when a glass of the same composition was quenched at an extremely fast rate of 10^5-10^6 K s^{-1}. In contrast, in this study the ^{27}Al MAS and especially the high-resolution 3QMAS spectra of glasses of similar composition and cooling rate of ca. 10^2-10^3 K s^{-1} show that all three of the Al^{IV}, Al^{V}, and Al^{VI} species are present in the structure, with Al^{IV} and Al^{V} being the most dominant ones. In fact the ^{27}Al MAS spectra of these normally cooled glasses as shown in Figure 9 look similar to that obtained for the glass with ca. 35 wt % Al_2O_3 in these previous studies when it was super-quenched at a rate of 10^5-10^6 K s^{-1}. [6,7] These results therefore put the validity of the hypothesis of cooling rate dependence of Al speciation in these glasses in question. To check this hypothesis in further detail the ^{27}Al MAS NMR spectrum of an aluminosilicate glass with 2 wt % Al_2O_3 is compared with that of a glass of same composition that has been drawn into a 125 μm diameter fiber at 2100 °C in a fiber draw-tower (Figure 10). The lack of any detectable difference between these two spectra indicates that Al speciation in this composition is independent of the cooling rate or fictive temperature of the glass.

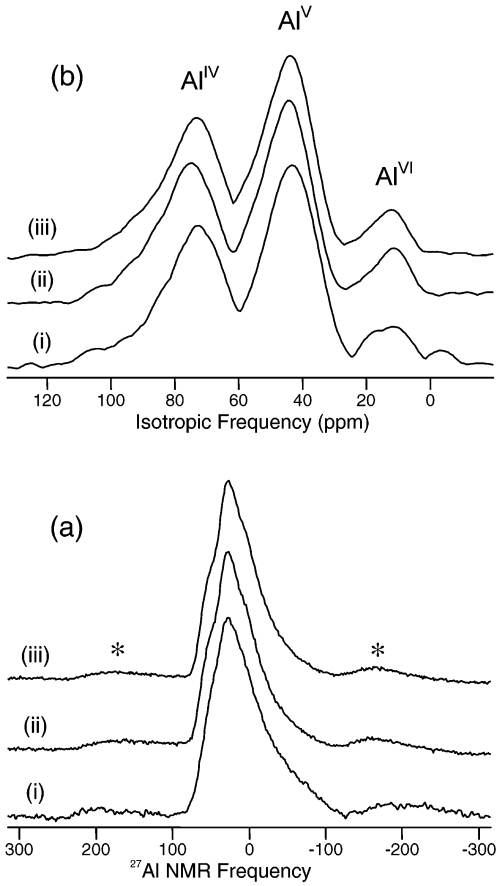

Figure 9. (a) ^{27}Al MAS NMR spectra of phase-separated binary aluminosilicate glasses with (i) 20, (ii) 30, and (iii) 40 wt % Al_2O_3. Asterisks denote spinning sidebands. (b) Isotropic projections of ^{27}Al 3QMAS NMR spectra of phase-separated binary aluminosilicate glasses containing (i) 20, (ii) 30, and (iii) 40 wt % Al_2O_3. The isotropic shift axis for these data was obtained after shearing the 3QMAS NMR spectra and correcting for the apparent Larmor frequency, as described in the experimental details.

Conclusions

The high-resolution ^{27}Al MAS and especially 3QMAS NMR spectroscopic results indicate that Al speciation in binary aluminosilicate glasses is strongly dependent on composition in the case of homogeneous glasses with ≤12 wt % Al_2O_3. Although all glasses in this composition range contain a mixture of Al^{IV}, Al^{V}, and Al^{VI}, three compositional regimes can be identified on the basis of Al speciation. Glasses with <1 wt %

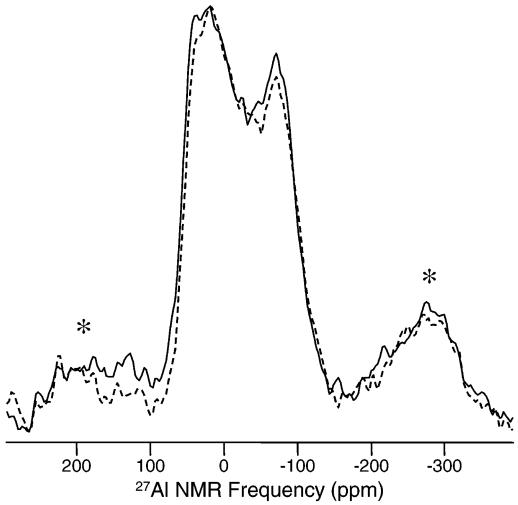

Figure 10. ^{27}Al MAS NMR spectra of a binary aluminosilicate glass with 2 wt % Al_2O_3 in slow-quenched bulk form (solid line) and fast-quenched fiber form (dashed line). Spinning sidebands are marked by asterisks.

Al_2O_3 contain mostly Al^{IV}, whereas Al^{IV} and Al^{VI} are the most dominant species in glasses with Al_2O_3 contents ranging between 1 and 7 wt %. A large fraction of the Al^{VI} sites in the latter group of glasses are strongly distorted and characterized by large C_q values similar to that observed in crystalline Al_2SiO_5 polymorphs, andalusite and sillimanite. Finally glasses with >7 wt % are characterized by the presence of Al^{IV} and Al^{V} as the dominant species, a trend that continues in phase-separated glasses with Al_2O_3 contents of up to 40 wt %. Phase-separated aluminosilicate glasses do not show any significant compositional dependence of Al speciation. Homogeneous aluminosilicate glasses do not show any significant dependence of Al speciation on fictive temperature. The ^{17}O 3QMAS NMR results indicate that addition of Al_2O_3 to silica does not result in the formation of typical nonbridging oxygens and Al−O−Al linkages and show the presence of Si−O−Al^{V} and Si−O−Al^{IV} sites besides the most abundant bridging oxygens of the type Si−O−Si. Addition of low-field strength alkali ions or high-field strength rare earth ions results in removal of the Al^{V} and Al^{VI} sites and charge balance and stabilization of the Al^{IV} sites. It is hypothesized that oxygen triclusters would form in glasses with <1 wt % Al_2O_3 where the relative concentrations of Al^{V} and Al^{VI} species are not sufficient to charge balance the Al^{IV} species. These glasses would therefore have a Si,Al−O tetrahedral network that is over-connected with respect to that in the case of pure silica or in any other oxide glasses for that matter. Such structural connectivity may be manifested in "super-strong" Al-doped silica glasses or liquids with higher viscosity than that of pure silica.

Acknowledgment. The authors would like to thank Ronald Parysek for the scanning electron microscopy work reported here and Ronald Andrus for his valuable technical assistance with sample preparation.

References and Notes

(1) Sen, S. *J. Non-Cryst. Solids* **2000**, *261*, 226.
(2) Sen, S.; Stebbins, J. F. *J. Non-Cryst. Solids* **1995**, *188*, 54.
(3) MacDowell, J. F.; Beall, G. H. *J. Am. Ceram. Soc.* **1969**, *52*, 17.
(4) Lægsgaard, J. *Phys. Rev. B* **2002**, *65*, 174104.
(5) Risbud, S. H.; Kirkpatrick, R. J.; Taglialavore, A. P.; Montez, B. *J. Am. Ceram. Soc.* **1987**, *70*, C-10.
(6) Sato, R. K.; McMillan, P. F.; Dennison, P.; Dupree, R. *J. Phys. Chem.* **1991**, *95*, 4483.
(7) Poe, B. T.; McMillan, P. F.; Angell, C. A.; Sato, R. K. *Chem. Geol.* **1992**, *96*, 333.
(8) Poe, B. T.; McMillan, P. F.; Coté, B.; Massiot, D.; Coutures, J.-P. *J. Phys. Chem.* **1992**, *96*, 8220.
(9) Schmücker, M.; MacKenzie, K. J. D.; Schneider, H.; Meinhold, R. *J. Non-Cryst. Solids* **1997**, *217*, 99.
(10) Jin, J.; Sakida, S.; Yoko, T.; Nogami, M. *J. Non-Cryst. Solids* **2000**, *262*, 183.
(11) Fujiyama, T.; Yokoyama, T.; Hori, M.; Sasaki, M. *J. Non-Cryst. Solids* **1991**, *135*, 198.
(12) Brower, K. L. *Phys. Rev. Lett.* **1978**, *41*, 879.
(13) Wang, S.; Stebbins, J. F. *J. Non-Cryst. Solids* **1998**, *231*, 286.
(14) Amoureaux, J.-P.; Fernandez, C.; Steuernagel, S. *J. Magn. Reson. A* **1996**, *123*, 116.
(15) Stebbins, J. F. Nuclear Magnetic Resonance Spectroscopy of Silicates and Oxides in Geochemistry and Geophysics. In *Handbook of Physical Constants*; Ahrens, T. J., Ed.; Americal Geophysical Union: Washington, DC, 1995; Vol. 2, p 303.
(16) Frydman, L.; Harwood, J. S. *J. Am. Chem. Soc.* **1995**, *117*, 5367.
(17) Amoureaux, J.-P.; Huguenard, C.; Engelke, F.; Taulelle, F. *Chem. Phys. Lett.* **2002**, *356*, 497.
(18) Schaller, T.; Stebbins, J. F. *J. Phys. Chem. B* **1998**, *102*, 10690.
(19) Stebbins, J. F.; Zhao, P.; Lee, S. K.; Oglesby, J. V. *J. Non-Cryst. Solids* **2001**, *293*−*295*, 67.
(20) Dirken, P. J.; Kohn, S. C.; Smith, M. E.; van Eck, E. R. H. *Chem. Phys. Lett.* **1997**, *266*, 568.
(21) Du, L.-S.; Stebbins, J. F. *J. Non-Cryst. Solids* **2003**, *315*, 239.
(22) Lacy, E. D. *Phys. Chem. Glasses* **1963**, *4*, 234.
(23) Saito, K.; Ogawa, N.; Ikushima, A. J.; Tsurita, Y.; Yamahara, K. *J. Non-Cryst. Solids* **2000**, *270*, 60.
(24) Sen, S.; Orlinskii, S. B.; Rakhmatullin, R. M. *J. Appl. Phys.* **2001**, *89*, 2304.
(25) Alemany, L. B.; Steuernagel, S.; Amoureaux, J.-P.; Callender, R. L.; Barron, A. R. *Solid State NMR* **1999**, *14*, 1.
(26) Ghose, S.; Tsang, T. *Am. Mineral.* **1973**, *58*, 748.
(27) Brown, I. D.; Shannon, R. D. *Acta Crystallogr.* **1973**, *A29*, 266.